J|A|C|S
ARTICLES
Published on Web 08/11/2006

Antimitotic Rhizoxin Derivatives from a Cultured Bacterial Endosymbiont of the Rice Pathogenic Fungus *Rhizopus microsporus*

Kirstin Scherlach,[†] Laila P. Partida-Martinez,[†] Hans-Martin Dahse,[†] and Christian Hertweck*[,†,‡]

Contribution from the Leibniz-Institute for Natural Product Research and Infection Biology (HKI), Jena, Germany, and Friedrich-Schiller-University, Jena, Germany

Received April 28, 2006; E-mail: christian.hertweck@hki-jena.de

Abstract: The potent antimitotic polyketide macrolide rhizoxin, the causal agent of rice seedling blight, is not produced by the fungus *Rhizopus microsporus*, as has been believed for over two decades, but by endosymbiotic bacteria that reside within the fungal mycelium. Here we report the successful isolation and large-scale fermentation of the bacterial endosymbiont ("*Burkholderia rhizoxina*") in pure culture, which resulted in a significantly elevated (10× higher) production of antimitotics. In addition to several known rhizoxin derivatives, numerous novel natural and semisynthetic variants were isolated, and their structures were fully elucidated. Cell-based assays as well as tubulin binding experiments revealed that methylated seco-rhizoxin derivatives are 1000−10000 times more active than rhizoxin and thus rank among the most potent antiproliferative agents known to date. Furthermore, more stable didesepoxy rhizoxin analogues were obtained by efficiently inhibiting a putative P-450 monooxygenase involved in macrolide tailoring.

Introduction

The mitotic spindle represents the prime target for arresting cell division and inducing apoptosis.[1−3] Its formation depends on a highly sensitive dynamic equilibrium, which, in a simplistic model, can be affected in two basic ways: either by blocking microtubule depolymerization (e.g. by paclitaxel, epothilone), or by binding to β-tubulin and thus inhibiting microtubule assembly (e.g. by the *Vinca* alkaloids, colchicine, and maytansine).[4] Not surprisingly, the most potent antimitotic compounds are represented by natural products, which have been biologically evaluated for defending the habitat, as efficient feeding deterrents, or as pathogenicity factors. Rhizoxin (**1**, Figure 1), the causal agent of rice seedling blight, is an important example for such an ecologically and pharmaceutically relevant antimitotic agent.[5,6]

About two decades ago, Iwasaki et al. succeeded in isolating the unprecedented polyketide macrolide **1** from cultures of the plant pathogenic fungus *Rhizopus microsporus*.[5,6] They demonstrated that rhizoxin alone induces an abnormal swelling of rice seedling roots, the typical symptoms of the plant disease,[7]

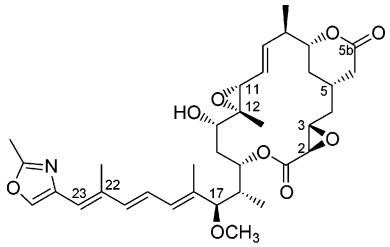

Rhizoxin (**1**)

Figure 1. Structure of rhizoxin, the causal agent of rice seedling blight and potent antitumoral agent.

at a concentration as low as 10 ng mL^{-1}.[6,8] In a subsequent study it was disclosed that rhizoxin inhibits rice cell division by binding to rice cell β-tubulin. The finding that rhizoxin also arrests mitosis in many other eukaryotic cells, including solid and hematologic tumors, has propelled an immense research endeavor.[9,10] As a result of the remarkable potency of rhizoxin against human and murine tumor cells and resistant sublines,[9] rhizoxin has undergone extensive clinical trials as a potential antitumor drug candidate.[11]

In the course of our studies on the rhizoxin biosynthetic machinery we made an unexpected observation. We discovered

[†] Leibniz-Institute for Natural Product Research and Infection Biology.
[‡] Friedrich-Schiller-University.

(1) Jordan, M. A.; Wilson, L. *Nat. Rev. Microbiol.* **2004**, *4*, 253.
(2) Hadfield, J. A.; Ducki, S.; Hirst, N.; McGown, A. T. *Prog. Cell Cycle Res.* **2003**, *5*, 309.
(3) Jordan, A.; Hadfield, J. A.; Lawrence, N. J.; McGown, A. T. *Med. Res. Rev.* **1998**, *18*, 259.
(4) Jordan, M. A. *Curr. Med. Chem.: Anti-Cancer Agents* **2002**, *2*, 1.
(5) Sato, Z.; Noda, T.; Matsuda, I.; Iwasaki, S.; Kobayashi, H.; Furukawa, J.; Okuda, S. *Ann. Phytopathol. Soc. Jpn.* **1983**, *49*, 128.
(6) Iwasaki, S.; Kobayashi, H.; Furukawa, J.; Namikoshi, M.; Okuda, S.; Sato, Z.; Matsuda, I.; Noda, T. *J. Antibiot.* **1984**, *37*, 354.
(7) Noda, T.; Hashiba, T.; Sato, Z. *Ann. Phytopathol. Soc. Jpn.* **1980**, *46*, 40.
(8) Iwasaki, S.; Namikoshi, M.; Kobayashi, H.; Furukawa, J.; Okuda, S.; Itai, A.; Kasuya, A.; Iitaka, Y.; Sato, Z. *J. Antibiot.* **1986**, *39*, 424.
(9) Tsuruo, T.; Oh-hara, T.; Iida, H.; Tsukagoshi, S.; Sato, Z.; Matsuda, I.; Iwasaki, S.; Okuda, S.; Shimizu, F.; Sasagawa, K.; Fukami, M.; Fukuda, K.; Arakawa, M. *Cancer Res.* **1986**, *46*, 381.
(10) Takahashi, M.; Iwasaki, S.; Kobayashi, H.; Okuda, S.; Murai, T.; Sato, Y. *Biochim. Biophys. Acta* **1987**, *926*, 215.
(11) Lafontaine, J. A.; Provencal, D. P.; Gardelli, C.; Leahy, J. W. *J. Org. Chem.* **2003**, *68*, 4215.

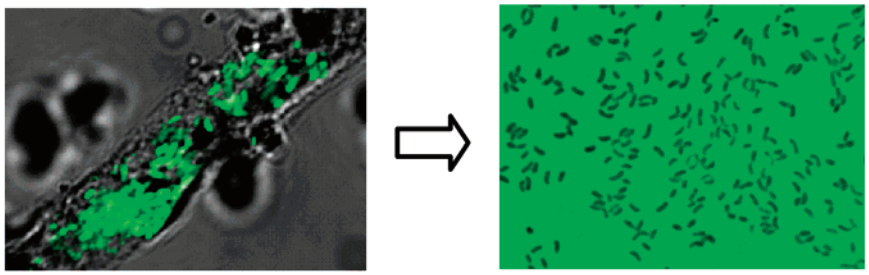

Figure 2. Rhizoxin-producing bacterial endosymbionts ("*Burkholderia rhizoxina*") in the mycelium of *Rhizopus microsporus* (left) and in pure culture (right).

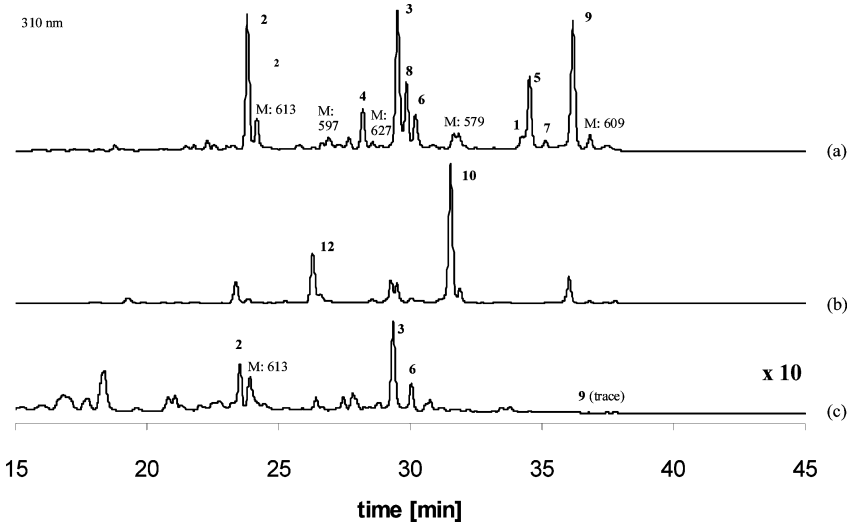

Figure 3. HPLC profiles of crude extracts from (a) cultivated endosymbionts ("*B. rhizoxina*" B4); (b) cultivated endosymbionts treated with ancymidol; and (c) *R. microsporus* HKI-315 (containing symbionts), 10× enlarged. (All extracts at a concentration of 2 mg mL^{-1} and monitored at 310 nm.)

that rhizoxin is not synthesized by the fungus, as has been assumed previously, but by bacteria living within the fungal mycelium.[12] In fact, these bacterial endosymbionts, which belong to the genus *Burkholderia*, could be detected in all studied rhizoxin-producing *Rhizopus* strains. Their role in rhizoxin production was unequivocally established by curing the fungus with an antibiotic, which resulted in a nonproducing strain. In addition, we were able to isolate a rhizoxin-producing bacterial strain from the fungus and to grow it in pure culture (Figure 2). These results unequivocally demonstrated that fungus and bacteria form an unparalleled symbiotic alliance against plants: the fungi harbor bacteria for the production of an antimitotic toxin, which weakens or kills the plant; the bacteria in return profit from the "safe" niche and from nutrients provided by the fungus.[12]

The cultivation of rhizoxin-producing bacterial endosymbionts could provide opportunities for sustainable production of this valuable antitumoral agent and for engineering rhizoxin biosynthesis.[13] Unfortunately, this first bacterial isolate (B1) obtained from *R. microsporus* (strain ATCC 62417) lost its ability to produce rhizoxin after its preservation was pursued.[12] Here we report the isolation and upscaled fermentation of a new "*Burkholderia rhizoxina*" isolate, yielding various rhizoxin derivatives with significantly improved antiproliferative activities.

Results and Discussion

By combining chemical and genetic analyses a *R. microsporus* strain collection comprising 15 different fungal isolates was screened for rhizoxin producers, and thus for bacterial−fungal symbioses. Using an optimized isolation protocol we succeeded in isolating, cultivating, and preserving six different endosymbiotic bacterial strains from eight individual rhizoxin-positive fungal samples. Symbionts were grown on TSB, nutrient agar, and VK medium, and their metabolite patterns were monitored by HPLC−MS. All isolates produced substantial quantities of the rhizoxin complex. Isolate B4, tentatively assigned as "*Burkholderia rhizoxina*" B4, from *R. microsporus* HKI-315 showed stable metabolite production and proved to be particularly well-suited for a scaled-up fermentation (14 L) and sustainable metabolite production.

Investigation of the extracts from the B4 and fungal cultures revealed not only that macrolide production is significantly (10×) higher than in the fungal fermentation (25 mg L^{-1} vs 2 mg L^{-1}) but also that the metabolic profile of the cultured symbiont is essentially devoid of unwanted metabolic background (Figure 3). Strikingly, about 40% of the crude extract is composed of rhizoxin derivatives. Apart from small quantities of **1**, a remarkable number of over 20 representatives of the rhizoxin complex were clearly detectable using an optimized HPLC−MS protocol (Figures 3 and 4). Major compounds were isolated by open column chromatography and repeated preparative HPLC. In all cases, UV absorbance maxima at 298, 310, and 324 nm indicated conjugated polyene systems, and IR

(12) Partida-Martinez, L. P.; Hertweck, C. *Nature* **2005**, *437*, 884.
(13) Sanders, I. R. *Nature* **2005**, *437*, 823.

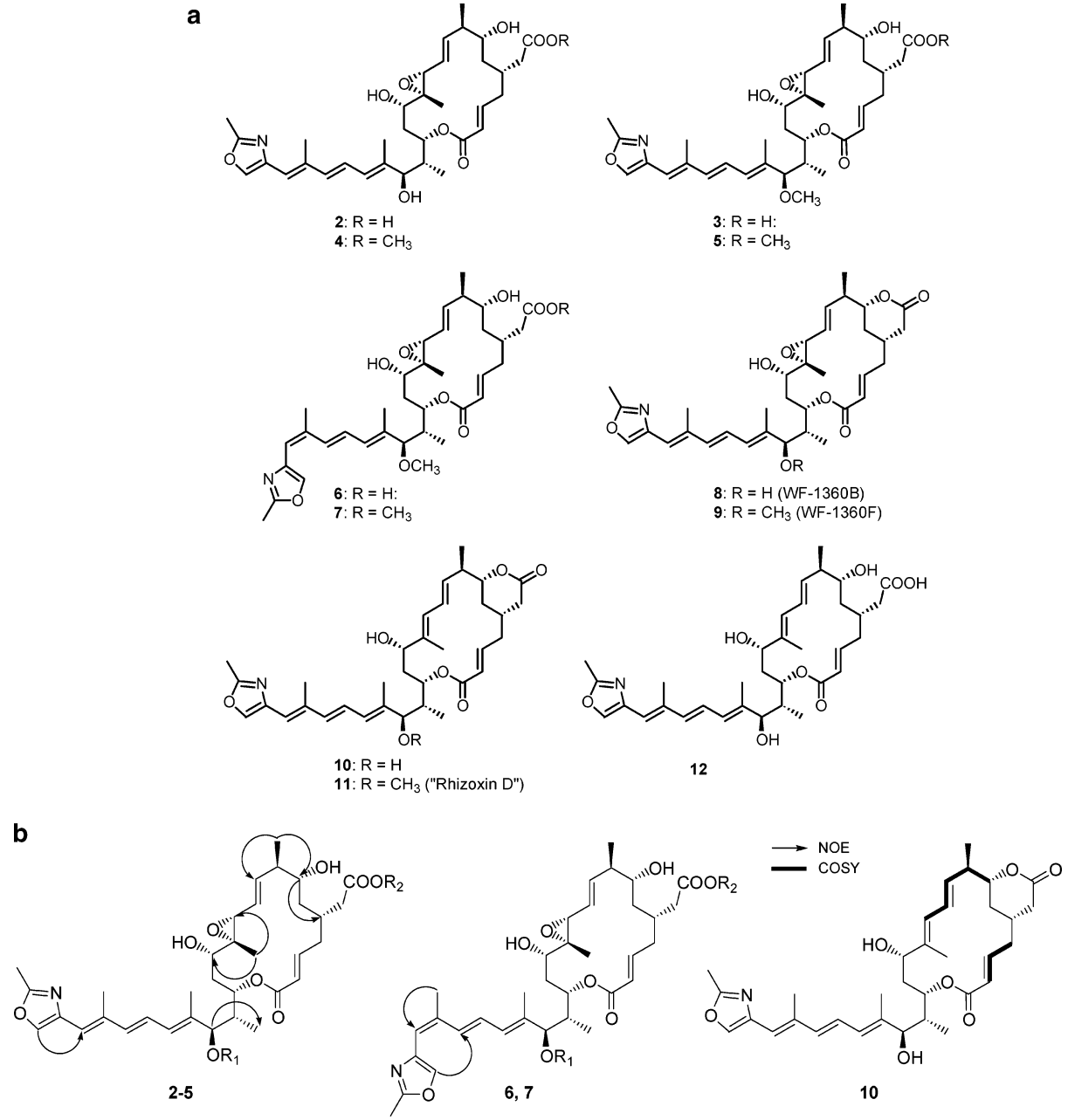

Figure 4. (a) Structures of rhizoxin derivatives produced by the cultivated symbiont and didesepoxy rhizoxin derivatives obtained from cytochrome P-450 monooxygenase inhibition. (b) Key NOE and COSY correlations of rhizoxins.

spectra revealed the presence of hydroxyl and carboxyl groups (ν_{max} = 3400 and 1700 cm^{-1}). Their structures were fully elucidated by 1D and 2D NMR measurements, and the relative configuration of the chiral centers was established by NOESY experiments (Figure 4b; ^1H and ^{13}C NMR data are shown in Tables 1 and 2 and in the Experimental Section).

The ESI-MS (positive ion mode) of **2** exhibited quasi-molecular ions at *m*/*z* 614 ($M + H^+$) and *m*/*z* 636 ($M + Na^+$). From HRESI-MS a molecular formula of $C_{34}H_{47}NO_9$ was deduced. ^1H and ^{13}C NMR data showed similarity to data obtained for **1**, suggesting the presence of a 16-membered lactone ring substituted at position 15 by a linearly conjugated tetraene system. This structure was corroborated by HMBC long-range coupling of H-15 and C-1 and vicinal couplings of the olefinic protons at 6.14 ppm (H-19), 6.65 ppm (H-20), and 6.40 ppm (H-21) as well as by HMBC long-range couplings between H-21 and C-23 and H-23 and C-25. Two olefinic carbon signals in the ^{13}C NMR spectrum (126.2 and 147.7 ppm) revealed **2** to be a 2,3-desepoxy derivative of **1**. Proton resonance at 3.13 ppm for H-7, a chemical shift of 73.9 ppm for C-7, and a carbon signal at 176.6 ppm (C-5b), indicative of a free carboxylic acid, established the structure of **2**. The structure of compound **3** was elucidated by comparison of its NMR data with those of **2**. The molecular formula ($C_{35}H_{49}NO_9$), deduced from HRESI-MS measurements, suggested the occurrence of an additional methyl group, which was supported by a carbon NMR signal at 56.6 ppm and the corresponding proton signal at 3.13 ppm. HMBC long-range coupling of H-17 and the additional carbon (56.6 ppm) disclosed *O*-methylation at position 17. Thus compound **3** was found to be identical with seco-rhizoxin 2a.[14]

Table 1. ^{1}H NMR Data of Novel Rhizoxin Derivatives

	δ_H (*J* [Hz])					
position	**2**	**4**	**5**	**6**	**7**	**12**
1						
2	5.78 d (15.6)	5.70 d (15.6)	5.67 d (15.6)	5.76 d (15.5)	5.77 d (15.6)	5.63 d (15.6)
3	6.79 ddd (15.5, 8.1, 7.5)	6.78 ddd (15.5, 9.0, 6.5)	6.74 ddd (15.5, 9.0, 6.6)	6.82 ddd (15.6, 8.4, 7.2)	6.78 ddd (15.6, 8.2, 7.6)	6.73 ddd (15.4)[b]
4	2.50 m[a]	2.40 m	2.39 m[a]	2.50 m	2.47 m	2.40 m
	2.15 m	2.06 m[a]	2.06 m	2.16 m	2.13 m	1.88 m[a]
5	2.24 m	2.21 m	2.21 m	2.30 m	2.28 m	1.89 m[a]
5a	2.50 dd[a]	2.52 dd (15.8, 6.9)	2.51 dd (15.8, 6.8)	2.52 m	2.52 dd (15.2, 5.6)	2.87 dd (15.4, 3.1)
	2.35 dd	2.35 d (6.9)	2.34 dd (15.7, 6.9)[a]	2.38 m	2.36 dd (15.2, 8.2)	2.18 m
5b						
6	1.75 m	1.75 dd (14.5, 5.9)	1.71 m	1.71 m	1.71 m	2.02 m[a]
	1.10 m	1.09 m	1.09 m	1.10 m	1.05 m	0.89 m
7	3.13 m	3.20 m	3.16 m	3.12 t (9.8)	3.11 m	3.01 t (9.6)
8	2.02 m[a]	2.03 m[a]	2.02 m	2.00 m	2.00 m[a]	1.98 m[a]
8a	1.02 d (6.0)[a]	1.03 d (6.6)	1.02 d (6.6)	1.03 d (6.6)	1.02 d (6.7)	1.01 d (6.5)
9	5.45 dd (15.6, 9.2)	5.51 dd (15.6, 9.4)	5.48 dd (15.6, 9.4)	5.43 dd (15.6, 9.3)	5.43 dd (15.6,9.3)	5.17 dd (15.1, 9.6)
10	5.16 dd (15.7, 8.1)	5.14 dd (15.6, 8.4)	5.12 dd (15.6, 8.4)	5.15 dd (15.6, 8.2)	15.16 dd (15.6, 8.2)	6.15 dd (15.2, 10.8)
11	3.00 (8.2)	3.16 d (8.5)	3.11 d[b]	2.98 d (8.2)	3.00 d (8.3)	5.68 (10.7)
12						
12a	1.29 s	1.33 s	1.31 s	1.29 s	1.29 s	1.71 s
13	2.96 dd (11.0, 2.7)	3.09 dd (10.2, 3.4)	3.00 dd (10.8, 2.8)	2.93 dd (10.8, 2.6)	2.94 dd (11.0, 2.6)	3.84 dd (10.8, 2.8)
14	2.03 m[a]	1.95 m[a]	1.94 m	2.02 m	1.95 m[a]	2.02 m[a]
	1.80 m	1.89 m	1.78 m	1.76 m	1.76 m	1.68 m
15	4.76 m	4.85 m	4.76 dd (9.9, 3.6)	4.74 dd (9.7, 3.4)	4.75 dd (9.7, 3.5)	4.75 m
16	2.05 m	1.98 m[a]	2.09 m	2.09 m	2.06 m	1.97 m
16a	0.99 d (6.5)[a]	0.94 d (6.8)	0.97 d (6.8)	1.00 d (6.8)	1.00 d (6.8)	0.98 d (6.8)
17	3.80 d (8.6)	3.88 d (6.0)	3.21 d (8.6)	3.34 d[b]	3.33 d (8.9)	3.80 d (8.5)
17-OCH_3			3.13 s	3.17 s	3.17 s	
18						
18a	1.89 s	1.83 s	1.82 s	1.84 s	1.84 s	1.89 s
19	6.14 d (10.9)	6.17 d (10.8)	6.06 d (10.8)	6.22 d (10.4)	6.22 d (10.9)	6.13 d (10.7)
20	6.65 dd (15.1, 10.8)	6.54 dd (15.1, 10.7)	6.57 dd (15.1, 10.7)	6.71 dd (15.3, 11.0)	6.71 dd (15.3, 11.0)	6.68 dd (15.1, 10.8)
21	6.40 d (15.2)	6.35 d (15.2)	6.34 d (15.2)	7.27 d (15.3)	7.27 d (15.3)	6.42 d (15.2)
22						
22a	2.09 s	2.11 s	2.12 s	2.04 s	2.04 s	2.11 s
23	6.21 s	6.22 s	6.23 s	6.09 s	5.78 s	6.21 s
24						
25	7.79 s	7.50 s	7.50 s	7.75 s	7.74 s	7.80 s
26						
26a	2.43 s	2.43 s	2.43 s	2.43 s	2.43 s	2.43 s
5b-OCH_3		3.68 s	3.67 s		3.67 s	

[a] Partial overlapping of signals. [b] Coupling was observed, but coupling constant not determined.

The ESI-MS (positive ion mode) of compound **6** showed the same quasi-molecular ions at *m*/*z* 628 ($M + H^+$) and *m*/*z* 650 ($M + Na^+$) as observed for **3**. In the proton spectrum a downfield shift of H-21 (6.44 ppm in **3** and 7.27 ppm in **6**) and an upfield shift of H-23 (6.23 and 6.09 ppm, respectively) were noticed. Observation of NOE correlation between H-25 and H-21 identified **6** as the (22*Z*) isomer of compound **3**. Finally, comparison of MS, IR, and NMR data of compound **9** to literature data suggested that it is identical with WF-1360F, respectively.[15] Unambiguous assignments were achieved by COSY, HMQC, and HMBC experiments.

It is remarkable that strain B4 produces primarily 2,3-desepoxyrhizoxin derivatives. However, also bis-epoxides as well as didesepoxy derivatives could be detected, albeit only in minute amounts. This is of particular interest as it has been suggested that in vivo hydrolysis of the epoxide moieties of rhizoxin may be responsible to some degree for its very short half-life in the body.[16] Thus didesepoxyrhizoxin derivatives, such as rhizoxin D (**11**), have become intriguing potential therapeutic agents and numerous synthetic approaches have been published in the past years.[17−24] In order to enlarge the fraction of didesepoxyrhizoxin derivatives produced by the symbiont we aimed at blocking epoxide formation by the addition of cytochrome P-450 monooxygenase inhibitors. Out of a number of inhibitors tested, ancymidol and metyrapone proved to be most efficient. Supplementation of a 1.5 L culture with ancymidol or the more affordable metyrapone (2.5 mM final

(14) Roberge, M.; Cinel, B.; Anderson, H. J.; Lim, L.; Jiang, X.; Xu, L.; Bigg, C. M.; Kelly, M. T.; Andersen, R. J. *Cancer Res.* **2000**, *60*, 5052.
(15) Kiyoto, S.; Kawai, Y.; Kawakita, T.; Kino, E.; Okuhara, M.; Uchida, I.; Tanaka, H.; Hashimoto, M.; Terano, H. *J. Antibiot.* **1986**, *39*, 762.
(16) McLeod, H. L.; Murray, L. S.; Wanders, J.; Setanoians, A.; Graham, M. A.; Pavlidis, N.; Heinrich, B.; ten Bokkel Huinink, W. W.; Wagener, D. J.; Aamdal, S.; Verweij, J. *Br. J. Cancer* **1996**, *74*, 1944.
(17) Williams, D. R.; Werner, K. M.; Feng, B. *Tetrahedron Lett.* **1997**, *38*, 6825.
(18) Keck, G. E.; Wager, C. A.; Wager, T. T.; Savin, K. A.; Covel, J. A.; McLaws, M. D.; Krishnamurthy, D.; Cee, V. J. *Angew. Chem., Int. Ed.* **2001**, *40*, 231.
(19) Mitchell, I. S.; Pattenden, G.; Stonehouse, J. *Org. Biomol. Chem.* **2005**, *3*, 4412.
(20) N'zoutani, M.-A.; Lensen, N.; Pancrazi, A.; Ardisson, J. *Synlett* **2005**, *3*.
(21) Jiang, Y.; Hong, J.; Burke, S. D. *Org. Lett.* **2004**, *6*, 1445.
(22) White, J. D.; Blakemore, P. R.; Green, N. J.; Hauser, E. B.; Holobski, M. A.; Keown, L. E.; Nylund Kolz, C. S.; Phillips, B. W. *J. Org. Chem.* **2002**, *67*, 7750.
(23) Mitchell, I. S.; Pattenden, G.; Stonehouse, J. P. *Tetrahedron Lett.* **2002**, *43*, 493.
(24) Kende, A.; Blass, B. E.; Henry, J. R. *Tetrahedron Lett.* **1995**, *36*, 4741.

Table 2. ^{13}C NMR Data of Novel Rhizoxin Derivatives

	δ_C					
position	**2**	**4**	**5**	**6**	**7**	**12**
1	167.0	165.7	165.1	166.9	166.9	167.7
2	126.2	124.6	124.9	125.9	126.2	124.6
3	147.7	147.1	146.4	148.3	147.6	150.2
4	36.8	37.7	37.5	37.3	36.8	39.9
5	32.8	32.2	32.1	33.0	33.0	36.3
5a	41.3	40.5	40.4	40.6	41.2	43.1
5b	176.6	173.5	173.5	177.6	174.8	178.7
6	39.2	37.9	37.8	39.7	39.1	38.6
7	73.9	74.3	74.2	73.9	73.9	78.2
8	46.8	45.5	45.5	46.8	46.8	47.5
8a	17.7	17.0	17.0	17.8	17.7	17.5
9	142.3	141.6	141.4	142.4	142.3	138.9
10	127.3	125.4	125.6	127.2	127.3	129.3
11	63.4	64.2	63.9	63.4	63.3	128.3
12	66.3	65.6	65.6	66.2	66.2	138.9
12a	11.2	11.1	11.1	11.2	11.2	10.8
13	79.5	78.2	78.3	79.5	79.5	79.6
14	34.0	33.1	31.8	33.9	34.0	33.9
15	75.3	74.1	73.3	74.8	74.9	74.6
16	41.4	40.3	39.4	40.6	40.6	41.6
16a	10.3	9.6	10.2	10.5	10.6	10.6
17	80.7	77.2	89.2	90.9	90.8	80.4
17-OCH_3			56.2	56.5	56.5	
18	140.7	138.2	136.3	138.4	138.3	140.9
18a	12.0	12.9	11.6	11.7	11.7	12.2
19	128.4	126.6	129.2	131.3	131.3	128.3
20	125.9	124.3	124.1	127.4	127.4	126.1
21	138.3	137.6	137.6	132.7	132.8	138.1
22	139.0	136.9	136.9	137.3	137.2	139.5
22a	14.7	14.4	14.3	21.0	21.0	14.7
23	120.9	120.5	120.7	118.7	118.8	120.8
24	139.5	138.8	138.7	139.1	139.1	139.0
25	137.7	135.9	135.9	138.1	138.1	137.7
26	162.9	160.9	160.9	163.2	163.2	162.9
26a	13.4	13.8	13.8	13.5	13.5	13.4
5b-OCH_3	-	51.7	51.7	-	52.0	-

concentration) significantly shifted the metabolic profile toward didesepoxyrhizoxin derivatives, as shown in Figure 5. Two members of the rhizoxin family (**10** and **12**) were isolated as major products. ^{13}C NMR spectra of **10** and **12** revealed the presence of two additional olefinic carbon signals for C-11 and C-12 instead of the epoxy signals in **2**. HMBC long-range couplings of H-9 and C-11 as well as H,H-COSY correlations of H-10 and H-11 established their structures. While **10** proved to be identical with rhizoxin derivative WF-1360C,[15] **12** represents the yet unknown corresponding seco derivative.

An initial activity screening revealed that the seco compound **3** exhibits a significantly elevated antiproliferative effect on K-562 leukemia cells compared to the δ-lactones. However, we also noted that the seco compounds are prone to spontaneous, nonenzymatic lactonization, which would result in a decrease in activity. For this reason we sought to hinder this unwanted reaction by means of esterification. Surprisingly, this goal was already achieved by simply dissolving the crude extract in methanol. HPLC−MS of the extract showed that several novel methylated rhizoxin derivatives (**4**, **5**, and **7**) were formed. For compound **4** a molecular formula of $C_{35}H_{49}NO_9$ was deduced from HRESI-MS measurements. The ^1H NMR spectrum showed an *O*-methyl-proton signal at 3.68 ppm (instead of the signal at 3.13 ppm in **3**). HMBC correlation of this signal with the carbon at 173.5 ppm established the partial structure of a methyl ester. Compound **5** with molecular formula $C_{36}H_{51}NO_9$ was likely to be the 17-*O*-methyl derivative of **4**. The NMR data of both compounds were in good accordance. Additional signals at 56.2 ppm in the ^{13}C NMR spectrum and at 3.13 ppm in the ^1H NMR spectrum and an upfield shift of H-17 (3.88 ppm in **4** to 3.21 ppm in **5**) supported the assumption. Observation of HMBC long-range coupling of H-17 and the carbon at 56.2 ppm as well as between H-5b and C-5b confirmed the connectivities. Compound **7** with molecular formula $C_{36}H_{51}NO_9$ was identified as the (22*Z*) isomer of compound **5**. Although compounds **4**, **5**, and **7** are simple semisynthetic derivatives of **1**, they represent some of the most potent antimitotic agents ever described. They exhibit significant potency against HeLa tumor cells (e.g. **4**: CC_{50} 1.7×10^{-2} μg/mL) and very strong antiproliferative effects on human K-562 leukemia cell lines (e.g. **4**: GI_{50} 5×10^{-7} μg/mL) and L-929 mouse fibroblast cell lines (e.g. **4**: GI_{50} 1.2×10^{-2} μg/mL).

All compounds isolated in this study were subjected to comprehensive biological testing. The data shown in Table 3 demonstrates that *Z*-isomers may be less active than the corresponding *E*-isomers, but there is no strict structure−activity relationship. The most surprising result is that some of the novel seco compounds—and in particular their methyl esters—are significantly more active than the corresponding δ-lactones. The antiproliferative assay using K-562 leukemia cells revealed femtomolar GI_{50} concentrations for rhizoxin methyl esters such as **4**, **5**, and **7**. Strikingly, these simple rhizoxin derivatives are thus 1000−10000 times more active than rhizoxin (see Table 3 and Figure 6) and rank among the most potent antimitotic agents known to date. Furthermore, it should be underlined that their CC_{50} (cytotoxic) and GI_{50} (antiproliferative) concentrations differ in up to 6 orders of magnitude (see Table 3 and Figure 6), which provides an ideal therapeutic window.

To investigate whether these high antiproliferative effects of the novel compounds (e.g. **4**) are in fact due to an interaction with the microtubule system, we evaluated them as inhibitors of tubulin polymerization using an in vitro microtubule assembly assay. The assay is based on the temperature-dependent equilibrium between α/β tubulin and microtubules. Assembly of microtubules is observed at 37 °C and can be monitored by recording the increase of absorbance at 360 nm due to the changing turbidity of the solution. Rapid cooling to 4 °C leads to depolymerization and a decrease of absorbance. By measuring the degree of polymerization the influence of tubulin effectors can be assessed. All compounds showed a pronounced effect on tubulin assembly, such as **4**, clearly establishing their role as antimitotic agents (Figure 7).

In conclusion, the bacterial endosymbionts of *R. microsporus* HKI-315 produce a battery of antimitotic compounds, which serve as pathogenicity factor for the fungus in suppressing cell division in rice seedling roots. In many other cases it has been suspected that natural products isolated from various eukaryotes, e.g. tunicates, sponges, plants, or insects, are in fact biosynthesized by associated bacterial symbionts.[25,26] Hard genomic evidence for this endosymbiont hypothesis has been provided by individual work groups in recent years.[27−30] However,

(25) Piel, J. *Nat. Prod. Rep.* **2004**, *21*, 519.
(26) Hildebrand, M.; Waggoner, L. E.; Lim, G. E.; Sharp, K. H.; Ridley, C. P.; Haygood, M. G. *Nat. Prod. Rep.* **2004**, *21*, 122.
(27) Piel, J. *Proc. Nat. Acad. Sci. U.S.A.* **2002**, *99*, 14002.
(28) Piel, J.; Hui, D.; Wen, G.; Butzke, D.; Platzer, M.; Fusetani, N.; Matsunaga, S. *Proc. Nat. Acad. Sci. U.S.A.* **2004**, *101*, 16222.
(29) Hildebrand, M.; Waggoner, L. E.; Liu, H.; Sudek, S.; Allen, S. W.; Anderson, C. M.; Sherman, D. H.; Haygood, M. G. *Chem. Biol.* **2004**, *11*, 1543.

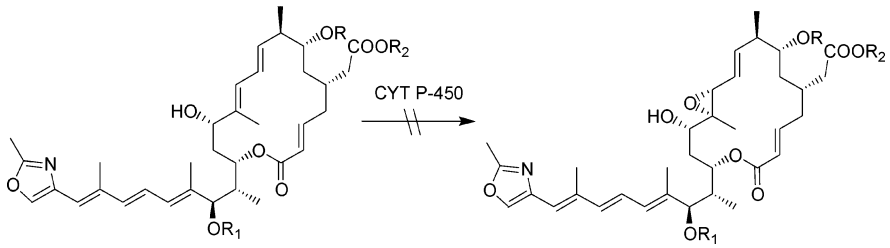

Figure 5. Blocking epoxide formation by cytochrome P-450 monooxygenase inhibition with ancymidol or metyrapone.

Table 3. Antiproliferative Effects of Rhizoxin Derivatives Compared to **1** and Colchicines

	GI_{50} [μg mL^{-1}]		CC_{50} [μg mL^{-1}]
compound	L-929	K-562	HeLa
1 (Rh.)	0.1	1.4×10^{-2} [a]	0.4
2 (Rh. S1)	0.1	1.5×10^{-2}	9×10^{-2}
3 (Rh. S2)	8×10^{-2}	1×10^{-6}	1.5×10^{-1}
4 (Rh. M1)	0.5	5×10^{-7}	1.7×10^{-2}
5 (Rh. M2)	0.5	$<5 \times 10^{-7}$	2×10^{-3}
6 (Rh. Z1)	0.2	1×10^{-2}	0.5
7 (Rh. Z2)	2×10^{-3}	5×10^{-7}	3.6×10^{-2}
9 (WF-1360F)	4.1×10^{-3}	2×10^{-3}	0.4
colchicine	0.9	0.02	0.01

[a] Reported antiproliferative activities for **1** (K-562, GI_{50}: 3.1×10^{-4} μg mL^{-1}).[9]

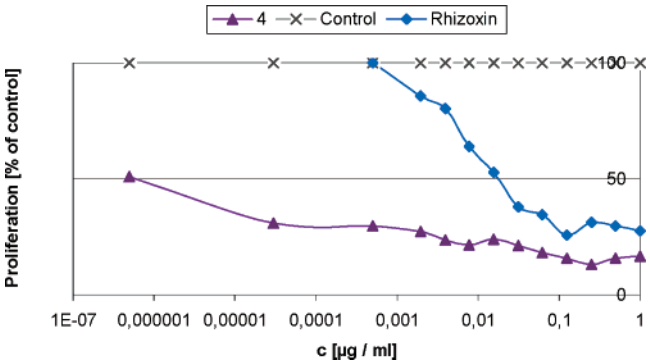

Figure 6. Antiproliferative effect of **4** compared to rhizoxin (**1**) on K-562 leukemia cells.

bacteria that live inside other organisms are notoriously difficult to cultivate on artificial media, and many are considered "nonculturable" (or "not yet culturable").[13,31] To the best of our knowledge, the sustainable production of eukaryont-derived metabolites by a cultured endosymbiont is unprecedented.[32] Here we report the first successful large-scale fermentation of a pure bacterial endosymbiont culture without its fungal host for metabolite production, yielding several novel antiproliferative rhizoxin derivatives. In addition, we were able to efficiently manipulate the rhizoxin pathway by cytochrome P-450 monooxygenase inhibition, which gave rise to more stable didesepoxyrhizoxin derivatives (**10** and **12**). In total, over 9 rhizoxin derivatives (out of which 6 are new) were isolated from upscaled endosymbiont fermentations, and their structures were fully assigned. Our studies demonstrate that the production and isolation of antimitotic rhizoxin derivatives can be greatly improved and manipulated by cultivating the bacterial endosymbionts. Extensive antimitotic bioassays also disclose novel

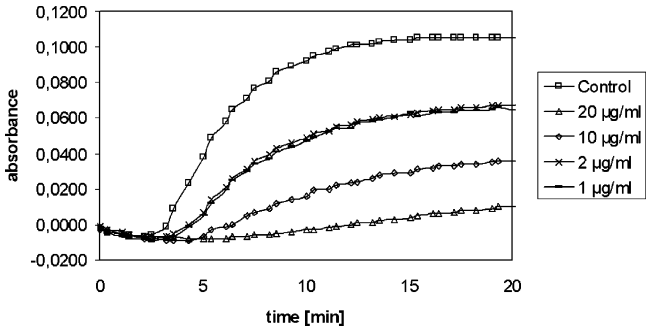

Figure 7. Effect of **4** on microtubule polymerization. Polymerization of tubulin at 37 °C was measured by recording the increase in absorbance at 360 nm. After a gap phase, the MTP polymerizes and the solution becomes turbid. After about 20 min, a steady-state level is reached, and no further increase in polymer mass is noticed. (It should be noted that compounds which efficiently decrease tubulin assembly powerfully suppress microtubule dynamics at around 100-fold lower concentrations and thus lead to cell cycle arrest at much lower concentrations.[1])

antiproliferative rhizoxin derivatives that are active at over 1000−10000 times lower concentrations than their natural progenitor, rhizoxin.

Experimental Section

General. NMR spectra were recorded on Bruker Avance DRX 500 and DPX 300 instruments. Spectra were referenced to the residual solvent signals. HPLC−MS measurements were recorded employing a Jasco HPLC with a UV detector (UV 970) and a reversed phase C18 column (Grom Sil 100 ODS 0AB, 3 μm, 250 × 4.6 mm) with gradient elution (MeCN/H_2O 25/75 5 min, in 35 min to MeCN/H_2O 80/20, in 5 min to 100% MeCN) coupled with a Finnigan LCQ benchtop mass spectrometer with an electrospray ion source and ion trap mass analyzer. HRESI-MS were recorded on a Finnigan MAT 95XL sector field mass spectrometer with a compatible ion source. IR and UV spectra were obtained using an FTIR spectrometer Satellite FTIR Mattson (Chicago, IL) and a Specord 200 photometer (Analytik Jena AG, Germany), respectively. Analytical HPLC was performed on a Shimadzu HPLC system consisting of an autosampler, high-pressure pumps, column oven, and DAD. HPLC conditions: C18 column (Grom Sil 100 ODS 0AB, 3 μm, 250 × 4.6 mm) and gradient elution (MeCN/0.1% TFA-(H_2O) 25/75 5 min, in 35 min to MeCN/0.1% TFA(H_2O) 80/20, in 5 min to 100% MeCN), flow rate 1 mL min^{-1}. Preparative HPLC was performed on a Shimadzu HPLC system with a UV detector. Optical rotation was measured using a 0.5 dm cuvette in a Propol Polarimeter (Dr. Kernchen, Seelze, Germany).

Bacterial Isolation. *R. microsporus* HKI-315 was cultivated at 30 °C and 80 rpm in VK medium composed of 1% corn starch, 0.5% glycerol, 1% gluten meal, 1% dried yeast, 1% corn steep liquor, and 1% $CaCO_3$, pH = 6.5. After 2 and/or 4 days, a small mycelial pellet (0.5 mL) was aseptically taken and submerged in 500 μL of 0.85% NaCl. Using mechanical stress (pipetting), the mycelium was broken and then submitted to centrifugation (30 min, 13 200 rpm). For each fungal strain, a loop of supernatant was then later plated in the following plates: nutrient agar, LB, TSA, and PDA—all media bought from

(30) Schmidt, E. W.; Nelson, J. T.; Rasko, D. A.; Sudek, S.; Eisen, J. A.; Haygood, M. G.; Ravel, J. *Proc. Nat. Acad. Sci. U.S.A.* **2005**, *102*, 7315−7320.
(31) Moran, N. A.; Wernegreen, J. J. *Trends Ecol. Evol.* **2000**, *15*, 321.
(32) Piel, J. *Curr. Med. Chem.* **2006**, *13*, 39.

Becton, Dickinson and Company. The different plates were incubated at 30 °C for several days, until the presence of mycelial or bacterial colonies could be confirmed. Once the first bacterial colonies appeared, they were picked up and cultivated in 1 mL of the corresponding liquid media at 30 °C and 150−200 rpm until growth could be seen, usually after 2−3 days. Then, this small grown culture was used to inoculate 10−20 mL at the same conditions. In liquid cultivations greater than 10 mL, growth was always monitored by means of a light microscope, by measuring the optical density (OD 600 nm) and the changes in pH. Rhizoxin production was confirmed by means of HPLC−MS.

Fermentation of "*Burkholderia rhizoxina*" Strain B4. From the bacterial cell bank, 100 μL of preserved bacteria (1:1 mixture of B4 in TSB and 30% glycerol) was used to inoculate 1 mL of fresh TSB. After 2 days of cultivation at 30 °C and 150 rpm, an aliquot of the grown culture (1 mL) was transferred to 20 mL of TSB. Once more, 2 days were required to get an optical density (600 nm) of about 0.5, and then this culture served as inoculum to prepare 300 mL seedling bacteria in TSB. Later, this preculture was used to inoculate 14 L of VK medium (1% corn starch, 0.5% glycerol, 1% gluten meal, 1% dried yeast, 1% corn steep liquor, and 1% $CaCO_3$, pH = 6.5) distributed equally in 28 Erlenmeyer flasks (1 L). Cultivation took place at 30 °C, 180 rpm, for 4 days.

Cytochrome P-450 Inhibition. Sixteen flasks containing 100 mL of VK medium were inoculated each with 10 mL of bacterial culture. Ancymidol or metyrapone, dissolved in 150 μL of DMSO, was added to 15 flasks to 2.5 mM final concentration at the time of inoculation; 150 μL of DMSO was added to the remaining flask as a control. The cultures were incubated for 4 days at 30 °C and 180 rpm. For extraction ethyl acetate was used.

Extraction and Isolation. The entire fermentation broth was exhaustively extracted with ethyl acetate, and the combined extracts were concentrated under reduced pressure. The crude extract (1 g) was fractionated by size exclusion chromatography on Sephadex LH-20 (eluent chloroform). Final purification of the rhizoxin derivatives was achieved by two steps of preparative RP-HPLC: (1) Nucleosil 100-7 250 × 40, flow rate 30 mL min^{-1}; (2) Eurospher 100-5 250 × 20, flow rate 12 mL min^{-1}, gradient MeCN/H_2O 25:75 for 5 min, leading to MeCN/H_2O 80:20 in 35 min, then 83% MeCN for 10 min, UV detection at 311 nm. For isolation of methyl esters methanol was used for isolation instead of chloroform.

Rhizoxin S1 (2): 20 mg. White amorphous powder. [α_D^{25} = +31 (*c* = 0.08 in MeOH). ^{1}H NMR (300 MHz) and ^{13}C NMR (75 MHz) in CD_3OD (see Tables 1 and 2). IR (ATR, solid film): $\tilde{\nu}$ = 2980, 2926, 2886, 1704, 1654, 1577, 1483, 1380, 1275, 1202, 1153, 1105, 1046, 963, 865, 827, 780, 746, 701 cm^{-1}. UV (MeOH): λ_{max} (log ϵ) = 299 (4.29), 310 (4.40), 324 nm (4.30). (+)-ESI-MS *m/z* 614 [M + H]$^+$, *m/z* 636 [M + Na]$^+$. HRESI-MS: *m/z* [M + Na]$^+$ = 636.3143 (calcd for $C_{34}H_{47}NO_9Na$ 636.3143).

Rhizoxin S2 (3): 100 mg. White amorphous powder. [α_D^{25} = +41 (*c* = 0.13 in MeOH). ^{1}H NMR (300 MHz, CD_3OD): δ 7.80 (s, 1H; H-25), 6.80 (ddd, *15.5, 8.1, 7.5*, 1H; H-3), 6.67 (dd, *15.2, 10.8*, 1H; H-20), 6.44 (d, *15.2*, 1H; H-21), 6.23 (s, 1H; H-23), 6.16 (d, *10.5*, 1H; H-19), 5.77 (d, *15.6*, 1H; H-2), 5.43 (dd, *15.6*, 9.3, 1H; H-9), 5.16 (dd, *15.7, 8.2*, 1H; H-10), 4.76 (dd, *9.9, 3.4*, 1H; H-15), 3.34 (d, 1H; H-17), 3.16 (s, 3H; 17-OCH_3), 3.12 (t, *10.0*, 1H; H-7), 2.99 (d, *8.2*, 1H; H-11), 2.94 (dd, *11.0, 2.7*, 1H; H-13), 2.51 (m, 1H; H-4α), 2.49 (m, 1H; H-5aα), 2.43 (s, 3H; H-26a), 2.33 (d, 1H; H-5aβ), 2.28 (m, 1H; H-5), 2.16 (m, 1H; H-4β), 2.10 (s, 3H, H-22a), 2.04 (m, 1H; H-16), 2.01−1.95 (m, 2H; H-8/H-14α), 1.83 (s, 3H; H-18a), 1.75 (m, 1H; H-14β), 1.71 (m, 1H; H-6α), 1.29 (s, 3H; H-12a), 1.07 (m, 1H; H-6β), 1.02 (d, *6.6*, 3H; H-8a), 1.00 (d, *6.8*, 3H; H-16a) ppm. ^{13}C NMR (75 MHz, CD_3OD) δ 176.8 (C-5b), 166.9 (C-1), 162.9 (C-26), 147.8 (C-3), 142.4 (C-9), 139.5 (C-24), 138.8 (C-21, C-22), 131.0 (C-19), 127.3 (C-10), 126.1 (C-2), 125.4 (C-20), 121.3 (C-23), 90.8 (C-17), 79.4 (C-13), 74.8 (C-15), 73.9 (C-7), 66.2 (C-12), 63.3 (C-11), 56.5 (17-OCH_3), 46.8 (C-8), 41.6 (C-5a), 40.6 (C-16), 39.2 (C-6), 36.8 (C-4), 33.9 (C-14), 32.8 (C-5), 17.7 (C-8a), 14.7 (C-22a), 13.4 (C-26a), 11.7 (C-18a), 11.2 (C-12a), 10.6 (C-16a) ppm. IR (ATR, solid film): $\tilde{\nu}$ = 2978, 2923, 2875, 1705, 1654, 1576, 1444, 1382, 1272, 1259, 1197, 1153, 1105, 1075, 1044, 1000, 969, 864, 826, 781, 704 cm^{-1}. UV (MeOH): λ_{max} (log ϵ) = 298 (4.42), 310 (4.52), 324 nm (4.39). (+)-ESI-MS *m/z* 628 [M + H]$^+$, *m/z* 650 [M + Na]$^+$. HRESI-MS: *m/z* [M + Na]$^+$ = 650.3271 (calcd for $C_{35}H_{49}NO_9Na$ 650.3300).

Rhizoxin M1 (4): 15 mg. White amorphous powder. [α_D^{25} = +32 (*c* = 0.1 in MeOH). ^{1}H NMR (300 MHz) and ^{13}C NMR (75 MHz) in $CDCl_3$ (see Tables 1 and 2). IR (ATR, solid): $\tilde{\nu}$ = 2977, 2935, 2924, 1705, 1652, 1577, 1437, 1377, 1260, 1202, 1152, 1105, 1048, 1007, 966, 863, 827, 780, 748, 702 cm^{-1}. UV (MeOH): λ_{max} (log ϵ) = 298 (4.27), 310 (4.35), 324 nm (4.23). (+)-ESI-MS *m/z* 628 [M + H]$^+$, *m/z* 650 [M + Na]$^+$. HRESI-MS: *m/z* [M + H]$^+$ = 628.3478 (calcd for $C_{35}H_{50}NO_9$ 628.3486).

Rhizoxin M2 (5): 91 mg. White amorphous powder. [α_D^{25} = +36 (*c* = 0.3 in MeOH). ^{1}H NMR (300 MHz) and ^{13}C NMR (75 MHz) in $CDCl_3$ (see Tables 1 and 2). IR (ATR, solid): $\tilde{\nu}$ = 3403, 2960, 2926, 1712, 1654, 1577, 1437, 1376, 1275, 1199, 1151, 1108, 1084, 1048, 1008, 971, 862, 827, 753, 706 cm^{-1}. UV (MeOH): λ_{max} (log ϵ) = 298 (4.56), 310 (4.67), 324 nm (4.54). (+)-ESI-MS *m/z* 642 [M + H]$^+$, *m/z* 664 [M + Na]$^+$. HRESI-MS: *m/z* [M + H]$^+$ = 642.3612 (calcd for $C_{36}H_{52}NO_9$ 642.3637).

Rhizoxin Z1 (6): 11 mg. White amorphous powder. [α_D^{25} = +116 (*c* = 0.07 in MeOH). ^{1}H NMR (300 MHz) and ^{13}C NMR (75 MHz) in CD_3OD (see Tables 1 and 2). IR (ATR, solid film): $\tilde{\nu}$ = 3348, 2931, 2875, 1698, 1684, 1654, 1569, 1559, 1436, 1376, 1272, 1202, 1182, 1137, 1049, 976, 865, 830, 801, 749, 722, 702 cm^{-1}. UV (MeOH): λ_{max} (log ϵ) = 298 (sh), 310 (4.55), 324 nm (4.43). (+)-ESI-MS *m/z* 628 [M + H]$^+$, *m/z* 650 [M + Na]$^+$. HRESI-MS: *m/z* [M + H]$^+$ = 628.3486 (calcd for $C_{35}H_{50}NO_9$ 628.3486).

Rhizoxin Z2 (7): 20 mg. White amorphous powder. [α_D^{25} = +138 (*c* = 0.15 in MeOH). ^{1}H NMR (300 MHz) and ^{13}C NMR (75 MHz) in CD_3OD (see Tables 1 and 2). IR (ATR, solid): $\tilde{\nu}$ = 3383, 2934, 2882, 1712, 1654, 1578, 1436, 1376, 1273, 1260, 1201, 1151, 1106, 1078, 1050, 1009, 974, 863, 828, 792, 781, 748, 705 cm^{-1}. UV (MeOH): λ_{max} (log ϵ) = 298 (4.26), 310 (4.32), 324 nm (4.21). (+)-ESI-MS *m/z* 642 [M + H]$^+$, *m/z* 664 [M + Na]$^+$. HRESI-MS: *m/z* [M + Na]$^+$ = 664.3434 (calcd for $C_{36}H_{51}NO_9Na$ 664.3456).

WF-1360F (9): 10 mg. White amorphous powder. [α_D^{25} = +84 (*c* = 0.18 in $CHCl_3$). ^{1}H NMR (300 MHz, $CDCl_3$) δ 7.51 (s, 1H; H-25), 6.80 (ddd, *15.6, 10.6, 5.1*, 1H; H-3), 6.58 (dd, *15.1, 10.7*, 1H; H-20), 6.35 (d, *15.2*, 1H; H-21), 6.24 (s, 1H; H-23), 6.07 (d, *10.7*, 1H; H-19), 5.67 (d, *16.0*, 1H; H-2), 5.54 (dd, *15.4, 9.8*, 1H; H-9), 5.32 (dd, *15.4, 9.2*, 1H; H-10), 4.60 (dd, *9.9, 3.1*, 1H; H-15), 3.73 (ddd, *12.0, 9.6, 2.8*, 1H; H-7), 3.24 (d, *9.2*, 1H; H-11), 3.22 (d, *5.0*, 1H; H-17), 3.15 (s, 3H; 17-OCH_3), 3.05 (dd, *10.6, 2.2*, 1H; H-13), 2.76 (m, 1H; H-5aα), 2.56 (m, 1H; H-4α), 2.45 (s, 3H; H-26a), 2.38 (m, 1H; H-16), 2.30 (m, 1H; H-8), 2.12 (s, 3H; H-22a), 2.08 (m, 1H; H-5aβ), 2.04 (m, 1H; H-14α), 1.95 (m, 1H; H-6aα), 1.87 (s, 3H; H-18a), 1.81 (m, 1H; H-14β), 1.79−1.72 (m, 2H; H-4β, H-5), 1.40 (s, 3H; H-12a), 1.17 (d, *6.5*, 3H; H-8a), 0.98 (d, *6.8*, 3H; H-16a), 0.71 (m, 1H; H-6β) ^{13}C NMR (75 MHz, $CDCl_3$) 169.9 (C-5b), 165.3 (C-1), 160.9 (C-26), 146.1 (C-3), 140.1 (C-9), 138.7 (C-24), 137.6 (C-21), 136.8 (C-22), 136.5 (C-18), 136.0 (C-25), 129.4 (C-19), 126.5 (C-10), 124.9 (C-2), 124.0 (C-20), 120.7 (C-23), 89.6 (C-17), 82.3 (C-7), 77.0 (C-13), 74.8 (C-15), 65.7 (C-12), 64.9 (C-11), 56.2 (17-OCH_3), 45.0 (C-8), 38.3 (C-16), 38.0 (C-4), 36.8 (C-5a), 33.9 (C-6), 31.7 (C-14), 29.7 (C-5), 16.6 (C-8a), 14.3 (C-22a), 13.8 (C-26a), 12.2 (C-12a), 11.5 (C-18a), 9.9 (C-16a). IR (ATR, solid film): $\tilde{\nu}$ = 3463, 2968, 2932, 2877, 1714, 1650, 1579, 1449, 1384, 1322, 1309, 1293, 1252, 1227, 1200, 1172, 1109, 1077, 1045, 982, 967, 877, 862, 829, 752, 702, 666 cm^{-1}. UV ($CHCl_3$): λ_{max} (log ϵ) = 302 (4.32), 314 (4.42), 328 nm (4.31). (+)-ESI-MS *m/z* 610 [M + H]$^+$, *m/z* 632 [M + Na]$^+$ HRESI-MS: *m/z* [M + H]$^+$ = 610.3396 (calcd for $C_{35}H_{48}NO_8$ 610.3374).

Rhizoxin D1 (WF-1360C, 10): 2.5 mg. White amorphous powder. ^{1}H NMR (300 MHz, $CDCl_3$) δ 7.54 (s, 1H; H-25), 6.78 (ddd, *15.7, 11.0, 4.6*, 1H; H-3), 6.59 (dd, *15.1, 10.*9, 1H; H-20), 6.38 (d, *15.2*, 1H; H-21), 6.26 (s, 1H; H-23), 6.23 (dd, *15.3*, *10.8*, 1H; H-10), 6.20 (d, *10.7*, 1H; H-19), 5.83 (d, *10.9*, 1H; H-11), 5.61 (d, *16.0*, 1H; H-2), 5.17 (dd, *15.2*, *9.7*, 1H; H-9), 4.68 (dd, *10.6*, *5.2*, 1H; H-15), 3.98 (dd, *10.8*, *2.8*, 1H; H-13), 3.89 (d, *6.3*, 1H; H-17), 3.68 (ddd, *12.0*, *9.6*, *2.7*, 1H; H-7), 2.75 (ddd, *2.1*, *5.5*, *17.9*, 1H; H-5aα), 2.55 (m, 1H; H-4α), 2.52 (s, 3H; H-26a), 2.28 (m, 1H; H-8), 2.20−2.05 (m, 2H; H-5aβ, H-14α), 2.10 (s, 3H; H-22a), 2.09 (m, 1H; H-16), 1.95 (m, 1H; H-6α), 1.87 (s, 3H; H-18a), 1.84 (m, 1H; H-14β), 1.81 (m, 1H; H-5), 1.78 (s, 3H; H-12a), 1.73 (m, 1H; H-4β), 1.19 (d, *6.4*, 3H; H-8a), 0.95 (d, *6.8*, 3H; H-16a), 0.68 (m, 1H; H-6β) (+)-ESI-MS *m*/*z* 580 $[M + H]^+$, *m*/*z* 602 $[M + Na]^+$ HRESI-MS: *m*/*z* $[M + Na]^+ = 602.3090$ (calcd for $C_{34}H_{45}NO_7Na$ 602.3094).

Rhizoxin D3 (12): 2.0 mg. White amorphous powder. ^{1}H NMR (300 MHz, CD_3OD) ^{13}C NMR (75 MHz, CD_3OD) (see Tables 1 and 2). (+)-ESI-MS *m*/*z* 598 $[M + H]^+$, *m*/*z* 620 $[M + Na]^+$ HRESI-MS: *m*/*z* $[M + H]^+ = 598.3399$ (calcd for $C_{34}H_{48}NO_8$ 598.3380).

Cytotoxicity, Antiproliferative, and Microtubule Assembly Assay. Cytotoxicity and antiproliferative assays were conducted as described previously.[33,34] Microtubule protein (MTP) from porcine brain was kindly provided by Prof. Dr. E. Unger and Dr. K. Böhm (FLI). The protein concentration of the solution was determined by the method of Lowry et al. with bovine serum albumin as standard. Microtubules were assembled in a buffer solution (20 mM PIPES, 80 mM NaCl, 0.5 mM $MgCl_2$, 1 mM EGTA) adding GTP (0.25 mM) and incubating samples at 37 °C. The polymerization was monitored by turbidity measurement at 360 nm using a Varian photometer. MTP concentration was 1.5 mg mL^{-1}. The drugs, dissolved in DMSO, were added to the cold MTP solution (2 °C). At the beginning of the measurement, temperature was raised to 37 °C; maximal absorbance was determined after 20 min. To prove reversibility of the polymerization and to discriminate between turbidity and unspecific protein precipitation, the samples were cooled to 2 °C afterward.

Acknowledgment. Financial support by the WGL is gratefully acknowledged. We also thank Ms. M.-G. Schwinger for assistance in fermentation, Ms. A. Perner for MS measurements, and Dr. F. A. Gollmick and Ms. F. Rhein for NMR measurements. We are grateful to Prof. Dr. E. Unger and Dr. K. Böhm (FLI) for kindly providing the microtubule protein.

JA062953O

(33) Ziehl, M.; He, J.; Dahse, H.-M.; Hertweck, C. *Angew. Chem.* **2005**, *117*, 4443.
(34) He, J.; Müller, M.; Hertweck, C. *J. Am. Chem. Soc.* **2004**, *126*, 16742.